

PAPER



Cite this: *Polym. Chem.*, 2015, **6**, 2133

One-pot synthesis and biological imaging application of an amphiphilic fluorescent copolymer *via* a combination of RAFT polymerization and Schiff base reaction

Zengfang Huang,^{a,b} Xiqi Zhang,^{b,c} Xiaoyong Zhang,^b Bin Yang,^b Yaling Zhang,^b Ke Wang,^b Jinying Yuan,^b Lei Tao^{*b} and Yen Wei^{*b}

In recent years, fluorescent organic nanoparticles (FONs) based on aggregation induced emission (AIE) dyes have received increasing attention for their potential in biology and biochemistry. In this contribution, a novel one-pot method for the fabrication of AIE-based FONs was developed *via* a combination of reversible addition–fragmentation chain-transfer (RAFT) polymerization and Schiff base reaction for the first time. During this procedure, an aldehyde functionalized hydrophobic tetraphenylethene AIE dye (named TPEA) reacted with the amine group of an amino-ended methacrylamide monomer by the Schiff base reaction, and the vinyl group in the monomer synchronously participated in RAFT polymerization together with a PEGMA monomer to form a new fluorescent copolymer. The as-prepared copolymer tended to self-assemble into FONs with the hydrophobic AIE core covered by a hydrophilic PEG shell, and the molar fractions of TPEA and PEG in the copolymer were about 20% and 80%, respectively, with 29 200 g mol^{−1} (*M_n*) and a narrow polydispersity index (PDI) (~1.30). The prepared amphiphilic copolymer nanoparticles (named TPEA-PEG) exhibited good fluorescence features and excellent dispersibility in aqueous solution. More importantly, these FONs presented a spherical morphology, uniform size (~100 nm), and excellent biocompatibility, making them promising candidates for bioimaging applications.

Received 21st December 2014,
Accepted 14th January 2015

DOI: 10.1039/c4py01769b

www.rsc.org/polymers

1. Introduction

The combination of different (catalytic) reactions into a one-pot system can not only avoid tedious intermediate purification steps, but also provide a powerful and exquisite strategy for sophisticated polymer synthesis and modification.^{1–5} Therefore, one-pot synthetic strategies have attracted increasing academic and industrial attention in polymer chemistry.^{6,7} For example, our group has developed a simultaneous one-pot synthesis methodology of functional polymers by combining three orthogonal reactions, namely click reaction, lipase-catalyzed transesterification and atom transfer radical polymerization (ATRP). These reactions were compatible and cooperated

well in a one-pot fashion, leading to well-defined new polymers with controllable molecular weights, compositions and functionalities.⁸ In our previous report, an almost neat Biginelli functionalized homopolymer has been successfully achieved in a one-pot fashion combining the Biginelli reaction and the RAFT polymerization.⁹ A one-pot strategy to fabricate the thermal responsive quantum dots (QDs)-poly(*N*-isopropylacrylamide) (PNIPAM) hybrid fluorescent microspheres has also been developed through 3-mercaptopropionic acid (MPA) capped CdTe QDs copolymerizing into PNIPAM microspheres during the monomer polymerization for the first time.¹⁰ Another one-step route to generate fluorescent functionalized carbon nanoparticles (F-CNPs) has also been developed by a hydrothermal method using different carbon sources with specific functional groups. The F-CNPs with diameters ranging from 5 to 30 nm possess high photoluminescence efficiency and are relatively monodispersed.¹¹ From a hydrophilic poly(ethylene oxide)-*block*-poly(acrylic acid) (PEO-*b*-PAA) macromolecular RAFT agent which is block-extended with styrene and a fluorescent 4,4-difluoro-4-bora-3a,4a-diaza-s-indacene (BODIPY) monomer, water-soluble and fluorescent core-shell nanoparticles (FNP) based on one-pot synthesis has been

^aCollege of Chemistry and Biology, Zhongshan Institute, University of Electronic Science & Technology of China, Zhongshan, 528402, P. R. China.
E-mail: hzf105@163.com

^bDepartment of Chemistry, the Tsinghua Center for Frontier Polymer Research, Tsinghua University, Beijing 100084, P. R. China.
E-mail: leitao@mail.tsinghua.edu.cn, weiyen@tsinghua.edu.cn

^cLaboratory of Bio-Inspired Smart Interface Science, Technical Institute of Physics and Chemistry, Chinese Academy of Sciences, Beijing, 100190, P. R. China

obtained in a miniemulsion RAFT polymerization, which are responsive to pH.¹² New molecules combining the functionalities of surface activity, polymerizability, and fluorescence properties within one molecule that could be seen as a fluorescent surfmer (surfactant and monomer) were successfully synthesized and utilized in one-pot production of fluorescent surface-labeled polymeric nanoparticles *via* miniemulsion polymerization.¹³

Schiff base compounds have attracted great research attention and have been widely applied in the fields of medicine, catalysis, analytical chemistry, *etc.* With many advantages, such as mild reaction conditions and high reaction rates, the Schiff base reaction was employed for protecting various functional groups and synthesizing a series of organic ligands.¹⁴ Meanwhile, by combining some polymerization methods, the Schiff base chemistry can provide an economic and convenient strategy to fabricate some functional polymers. An inexpensive, biocompatible self-healing hydrogel as a new injectable cell therapy carrier has been facilely developed through a Schiff-base crosslinked chitosan by our group, that dynamic hydrogel could self-heal itself automatically without additional assistance.^{15,16} Based on the work of Bentley and co-workers regarding reductive amination,^{17,18} another strategy was developed by Haddleton's group to synthesize an aldehyde functionalized branched PEG polymer by ATRP and then conjugated to proteins by the Schiff base reaction.^{19,20} Furthermore, a core-shell structure can also be achieved within a single molecule with a hyper-branched conjugated AIE polymer core and poly(ethylene glycol) arms through the acylhydrazone connection *via* Schiff-base chemistry.^{21,22} Some aldehyde-functional polycarbonates (PCs) have been fabricated *via* ozonolysis and reductive work-up of allyl-functional PCs. The resulting aldehydes were functionalized with amino-oxy compounds under mild conditions through Schiff base linkages.²³ A novel double-hydrophilic block copolymer poly(2-(2'-methoxyethoxy)-ethyl methacrylate-*co*-oligo(ethyleneglycol) methacrylate)-*b*-poly(2-aminoethyl ethacrylate) (P(MEO₂MA-*co*-OEGMA)-*b*-PAMA) has been successfully synthesized by two-step RAFT polymerization. Then, the amino groups of PAMA blocks in the copolymers react with 1-pyrenecarboxaldehyde *via* the Schiff-base reaction, and the resulting copolymers are self-assembled to form spherical micelles in aqueous solution.²⁴

In the last decade, fluorescent molecules and nano-objects have received increasing attention for their potential in biology and biochemistry, which are especially attractive for sensing, imaging and biomedical applications.²⁵ Owing to its good biocompatibility, low immunogenicity, and high water solubility, polyethylene glycol (PEG), a type of hydrophilic polymer, has been regarded as one of the best choices for surface modification of both inorganic and organic nanoparticles.²⁶ When a polymerizable AIE dye is employed in the polymerization of poly(ethylene glycol) monomethacrylate (PEGMA) by RAFT polymerization, the obtained amphiphilic polymers can be readily self-assembled into AIE-based FONs between 100 and 200 nm and exhibit high water dispersibility, intense fluorescence, and excellent biocompatibility.^{27–30} As a class of

well-known AIE material, tetraphenylethene (TPE) derivatives have been widely developed for chemosensor and biomedical applications.^{31,32} In this study, a novel one-pot strategy of a smart combination of RAFT polymerization and *in situ* Schiff base reaction for fabrication of an AIE-based copolymer was developed for the first time. The Schiff base reaction between an amine donor monomer of *N*-(3-aminopropyl) methacrylamide (APMA) and AIE-based tetraphenylethene-benzaldehyde (TPEA) formed the target monomer TPEA-MA. New monomers such as TPEA-MA obtained by this method synchronously participated in RAFT polymerization together with PEGMA to form a new amphiphilic copolymer with transformed fluorescent side groups, which tended to self-assemble into FONs in aqueous solution. To study the cell imaging application, the dispersibility, AIE property, and biocompatibility of the as-prepared copolymer were subsequently investigated.

2. Experimental

2.1. Materials and characterization

Poly(ethylene glycol) monomethacrylate (PEGMA, $M_n = 500$, J&K Chemical, AR), 2,2'-azobisisoheptonitrile (AVBN, J&K Chemical, 98%), *N*-(3-aminopropyl) methacrylamide (APMA, Tongchuang Pharma Co., Ltd, 98%), and triethylamine (TEA, J&K Chemical, AR) were all used as purchased. Tetraphenylethene-benzaldehyde (TPEA) and the chain transfer agent (CTA) of 4-cyano-4-(ethylthiocarbonothioylthio) pentanoic acid were prepared according to the literature methods.^{33–35}

Gel permeation chromatography (GPC) analysis of the copolymer was performed using *N,N*-dimethyl formamide (DMF) as the eluent. The GPC system was a Shimadzu LC-20AD pump system consisting of an auto injector, a MZ-Gel SDplus 10.0 mm guard column (50 × 8.0 mm, 10² Å) followed by an MZ-Gel SDplus 5.0 mm bead-size column (50–10⁶ Å, linear) and a Shimadzu RID-10A refractive index detector. The system was calibrated with narrow molecular weight distribution polystyrene standards ranging from 200 to 10⁶ g mol⁻¹. A ¹H NMR spectrum was obtained using a JEOL JNM-ECA 400 (400 MHz) spectrometer with tetramethylsilane (TMS) as a reference. An UV-vis absorption spectrum was recorded on a Perkin-Elmer LAMBDA 35 UV/vis system. Fluorescence spectra were recorded on a PE LS-55 spectrometer with a slit width of 3 nm for the emission of TPEA-PEG in water or in THF solution. The FT-IR spectra were obtained in reflection mode on a Perkin-Elmer Spectrum 100 spectrometer (Waltham, MA, USA). Typically, 4 scans at a resolution of 1 cm⁻¹ were accumulated to obtain one spectrum. Transmission electron microscopy (TEM) image was recorded on a JEM-1200EX microscope operated at 100 kV, the TEM specimens were prepared by placing a drop of the TPEA-PEG suspension on a carbon-coated copper grid.

2.2. One-pot synthesis of a fluorescent copolymer

The procedure for the one-pot synthesis of the fluorescent copolymer TPEA-PEG is as follows: APMA (38 mg, 0.216 mmol), TPEA (94 mg, 0.216 mmol), PEGMA (323 mg,

0.646 mmol), TEA (30 mg, 0.290 mmol), CTA (2.8 mg, 0.01 mmol), AVBN (1.2 mg, 0.005 mmol) and 1.0 mL mixed solvent of acetonitrile–methanol–THF (v/v/v = 1/1/1) were introduced into a Schlenk tube with a magnetic stir bar, and then followed by the freeze–pump–thaw cycle three times. The Schlenk tube with the reaction mixture was put into an oil bath maintained at 55 °C for 36 h. At the end of polymerization, the mixed solvent was removed with the rotary evaporator. The purified copolymer was obtained *via* precipitation from THF to petroleum ether three times, and then dried under vacuum for further characterization (yield: 0.29 g). Finally, a 10 mg TPEA-PEG copolymer was added to 5 mL H₂O, then shaken until it dissolved completely, which was used to investigate its self-assembly.

2.3. Cytotoxicity of TPEA-PEG FONs

The effects of TPEA-PEG FONs on A549 cells were examined by the observation of cell morphology.^{36,37} In brief, cells were seeded into 6-well microplates in 2 mL of respective media containing 10% fetal bovine serum (FBS) at a density of 1×10^5 cells mL⁻¹. After cell attachment, plates were washed with PBS and cells were treated with a complete cell culture medium, or different concentrations of TPEA-PEG FONs prepared in 10% FBS containing media for 24 h. Then all samples were washed with PBS three times to remove the uninternalized FONs. An optical microscope (Leica, Germany), with $\times 100$ magnification was used to observe the morphology of cells.

The cell viability of TPEA-PEG FONs on A549 cells was evaluated by a cell counting kit-8 (CCK-8) assay on the basis of our previous reports.^{38,39} In brief, cells were seeded in 96-well microplates with 160 μ L of respective media containing 10% FBS at a density of 5×10^4 cells mL⁻¹. After cell attachment for 24 h, the cells were incubated with 10, 20, 40, 80, 120 μ g mL⁻¹ TPEA-PEG for 8 and 24 h. After the nanoparticles were removed, the cells were then washed with PBS three times. 10 μ L of CCK-8 dye and 100 μ L of DMEM cell culture medium were added into each well and incubated for 2 h at 37 °C. Then the plates were analyzed using a microplate reader (Victor III, Perkin-Elmer). The absorbance of formazan dye was obtained at 450 nm, with the reference wavelength at 620 nm. The absorbance values were proportional to the number of live cells. The percent reduction of the CCK-8 dye was compared to controls (cells not exposed to TPEA-PEG FONs), which represented 100% CCK-8 reduction. The microplate experiment was repeated three times with three replicate wells. Cell survival is expressed as absorbance relative to that of untreated controls, and the results are presented as mean \pm standard deviation (SD).

2.4. Confocal microscopic imaging (CLSM) of cells using TPEA-PEG FONs

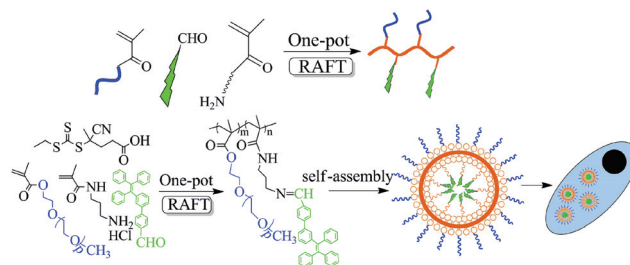
The confocal microscopic imaging was used to evaluate the cell uptake of TPEA-PEG FONs.^{15,40} In brief, cells were seeded in a glass bottom dish with a density of 1×10^5 cells per dish. On the day of treatment, the cells were incubated with TPEA-PEG FONs at a final concentration of 20 μ g mL⁻¹ for 3 h

at 37 °C. Subsequently, to remove the TPEA-PEG FONs, the cells were washed three times with PBS and then fixed with 4% paraformaldehyde for 10 min at room temperature. Cell images were obtained using a confocal laser scanning microscope Zeiss 710 3-channel (Zeiss, Germany) with an excitation wavelength of 405 nm.

3. Results and discussion

In aqueous solution, the pH value of the solution significantly affects the reactivity of the Schiff base. Generally, higher acidity destroys the Schiff base, while the Schiff base becomes relatively stable in alkaline solution.¹⁴ In this contribution, we have reported a straightforward one-pot synthetic method through the combination of RAFT polymerization and *in situ* Schiff base monomer transformation. As Et₃N was added to maintain the alkalinity of the solution, the target monomer (TPEA)-methacrylate (TPEA-MA) was facily prepared by the Schiff base reaction between the amino-containing monomer APMA and aldehyde-functionalized TPEA with excellent fluorescence. The as-prepared new monomer TPEA-MA together with PEGMA synchronously participated in RAFT polymerization to form a new copolymer with transformed fluorescent side groups. The introduction of TPEA and hydrophilic PEG would respectively endow the copolymer with fluorescence and excellent water solubility, thus the obtained water-soluble fluorescent copolymer was expected to self-assemble into nanoparticles and internalized by cells. The synthetic strategy in the current report is schematically illustrated in Scheme 1.

The number average molecular weight (M_n) of the finally obtained copolymer was about 29 200 g mol⁻¹ with a narrow PDI (~ 1.30 , Fig. 1A). The ¹H NMR spectrum of the copolymer is also determined and shown in Fig. 1B. The characteristic peak of the ester group of the PEGMA can be clearly observed at 4.05 ppm, and the aromatic hydrogen peak of TPEA appears clearly in the range of 7.12–7.87 ppm. The –N=CH– group in the Schiff base product is found to locate at 8.29 ppm, confirming the successful incorporation of TPEA into the copolymer. Depending on the integral ratio of the peaks at 8.29 ppm and 4.05 ppm, the molar fractions of TPEA and PEG in the copolymer can be calculated as approximately 20% and 80%, respectively.



Scheme 1 Schematic showing one-pot synthesis of TPEA-PEG copolymers through RAFT polymerization and the Schiff base reaction, and then self-assembly of these copolymers for cell imaging.

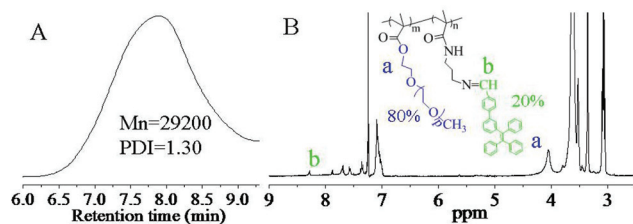


Fig. 1 (a) The GPC trace (DMF) and (b) ^1H NMR spectrum (CDCl_3) of the finally obtained fluorescent copolymer.

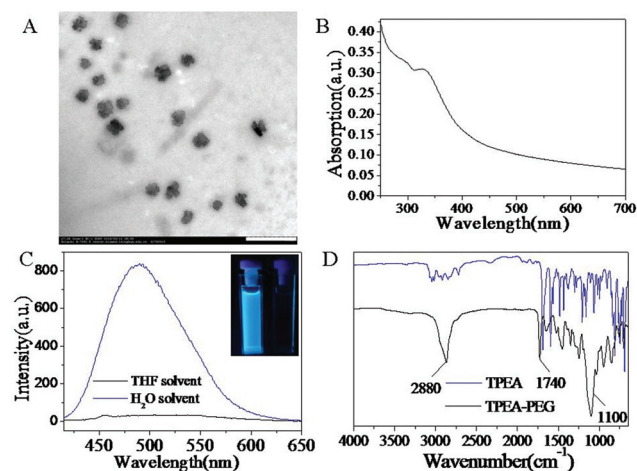


Fig. 2 Characterization of TPEA and TPEA-PEG FONs: (A) TEM image of TPEA-PEG FONs dispersed in water, scale bar = 500 nm; (B) UV-Vis spectrum of TPEA-PEG FONs dispersed in water; (C) fluorescence emission spectra of TPEA-PEG FONs in water (left cuvette) and THF (right cuvette), inset is the fluorescent image of TPEA-PEG FONs taken at 365 nm UV light; (D) FT-IR spectra of TPEA and TPEA-PEG.

The characterization information of the obtained TPEA-PEG FONs is depicted in Fig. 2. Transmission electron microscopy (TEM) image in Fig. 2A shows that the TPEA-PEG copolymer can self-assemble into uniform spherical nanoparticles with about 100 nm diameter. The self-assembly of the copolymer into spherical nanoparticles further confirmed that TPEA and PEGMA were successfully incorporated into the copolymer *via* the Schiff base reaction and RAFT polymerization. Fig. 2B describes the UV absorption spectrum of TPEA-PEG FONs dispersed in water, and the entire spectrum starts to increase with absorption from 700 nm, indicating the formation of nano-aggregates in the solution.⁴¹ The light scattering, or Mie effect, of the nanoparticle suspensions in the solution effectively decreased light transmission and caused the apparent high absorption and levelling-off of the tail in the visible region. For the entire spectrum, the maximum absorption wavelength is located at 350 nm, which might contribute to the electron transition $\pi \rightarrow \pi^*$ because TPEA-PEG copolymers have the π - π conjugated structure. Owing to the surface of the amphiphilic TPEA-PEG copolymer covered by hydrophilic PEG, they tended to self-assemble into nanoparticles in aqueous solution, forming PEGylated AIE-based FONs, so that the

obtained FONs could be well dispersed in pure aqueous solution. On the other hand, the TPEA-PEG FONs were endowed with the AIE property because the hydrophobic AIE dye (TPEA) in the core of FONs would partly aggregate in aqueous solution.⁴² However, both TPEA-MA and PEGMA can dissolve in some organic solvents, making the obtained TPEA-PEG polymer to have excellent dissolution in an organic solvent than in water. Fig. 2C shows the fluorescence difference between water and THF; the fluorescent property is clearly observed along with the maximum emission peak at 490 nm in the aqueous solution, while in the THF solution, almost no fluorescence is observed, indicating the obvious AIE property. A possible explanation for this phenomenon is that in organic solutions, the intramolecular rotation is active, which serves as a relaxation channel for the excited state to decay, while in the aggregates, the rotation is restricted due to the physical constraint, which blocks the non-radiative path and activates the radiative decay.^{43,44}

Fig. 2D shows the FT-IR spectra of TPEA and TPEA-PEG copolymers. A series of absorbance bands of TPEA located between 1400 and 1600 cm^{-1} assigned to the stretching vibration of the polycyclic aromatic rings of TPEA can be observed. The C-H stretching vibration of polycyclic aromatic rings of TPEA presents at 2700–3100 cm^{-1} ; moreover, two characteristic peaks of C=O and C=C located at 1710 and 1610 cm^{-1} can also be clearly observed. For the spectrum of TPEA-PEG, the C-H band of $-\text{CH}_2-$, $-\text{CH}_3$ and polycyclic aromatic rings located at 2880 cm^{-1} can also be clearly observed and the peak located at 1740 cm^{-1} is ascribed to the C=O stretching vibration. As compared with the spectrum of the TPEA dye, the peak of the TPEA-PEG copolymer located at 1710 cm^{-1} almost disappeared, indicating the successful incorporation of TPEA into the copolymer by the Schiff base reaction. On the other hand, the spectra of the TPEA-PEG copolymer exhibits one characteristic peak of 1100 cm^{-1} (stretching vibration of C-O), further confirming the successful incorporation of PEGMA into the copolymer through RAFT polymerization. A combination of hydrophobic TPEA and hydrophilic PEG, the amphiphilic TPEA-PEG copolymer easily tends to self-assemble into uniform FONs in the aqueous solution with the hydrophobic TPEA core covered by the hydrophilic PEG segments.

The biocompatibility of TPEA-PEG FONs was further evaluated by cell incubation with different concentrations of FONs for up to 24 h as shown in Fig. 3A–C. The optical microscopy observation results indicate that cells maintain their normal morphology. Even when the concentration of TPEA-PEG FONs is as high as 80 $\mu\text{g mL}^{-1}$, the cell morphology does not change clearly, implying the good biocompatibility of TPEA-PEG FONs. The good biocompatibility of TPEA-PEG FONs was further confirmed through A549 cell viability with a cell counting kit-8 (CCK-8) assay as shown in Fig. 3D. The result demonstrates that the values of cell viability are more than 90%, when the cells are incubated with 10–120 $\mu\text{g mL}^{-1}$ of TPEA-PEG FONs. Moreover, decrease of cell viability is not clearly observed even when the concentration of TPEA-PEG

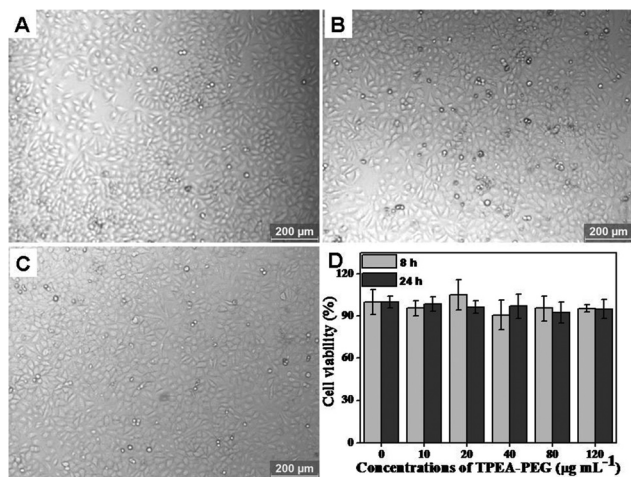


Fig. 3 Biocompatibility evaluation of TPEA-PEG FONs. (A–C) Optical microscopy images of A549 cells incubated with different concentrations of TPEA-PEG FONs for 24 h. (A) control cells, (B) $20 \mu\text{g mL}^{-1}$, (C) $80 \mu\text{g mL}^{-1}$, (D) cell viability of TPEA-PEG FONs with A549 cells. The biocompatibility evaluation suggested that TPEA-PEG FONs were biocompatible enough for biomedical applications.

FONs increases to $120 \mu\text{g mL}^{-1}$. From the above results, it can be concluded that TPEA-PEG FONs have good biocompatibility with cells and are promising candidates for biomedical applications.

Due to the excellent water dispersibility, good fluorescence features and favorable biocompatibility, the cell uptake behavior of TPEA-PEG FONs by CLSM was used to further investigate their potential cell imaging applications as shown in Fig. 4A–C. After the cells were incubated with $20 \mu\text{g mL}^{-1}$ of TPEA-PEG FONs for 3 h, strong fluorescence at the cytoplasm could be clearly observed; however, the areas with relatively weak fluorescence intensity could be the location of the cell nucleus (Fig. 4B).⁴⁵ These preliminary results suggest that TPEA-PEG FONs can be easily taken up by cells and are mainly located at the cytoplasm. As compared with the size of FONs and nucleus pores, these FONs were considered to be taken up by endocytosis of the cells.⁴⁶ Based on the results of cell viability, we believe that TPEA-PEG FONs, combining the merits of AIE and PEG are biocompatible enough for bioimaging applications. More importantly, due to the controllability of RAFT polymerization and the convenience of the Schiff base reaction, novel

monomers from the Schiff base reaction can also be facilely integrated into polymer chains, thus multifunctional imaging and theranostic platforms can be obtained by controllable polymerization of the AIE monomer from the Schiff base reaction. Considering the excellent fluorescence and amphiphilic properties, these FONs are promising candidates for biomedical applications.

4. Conclusions

In conclusion, we have developed a novel one-pot strategy for the fabrication of TPEA-PEG FONs through controllable RAFT polymerization and the Schiff base reaction of APMA and functional AIE dye (TPEA) for the first time. The M_n of the as-prepared copolymer was about $29\,200 \text{ g mol}^{-1}$ with a narrow PDI (~ 1.30), and the molar fractions of TPEA and PEG segments in the copolymer were about 20% and 80%, respectively. In aqueous solution, these amphiphilic TPEA-PEG copolymers showed excellent water dispersibility owing to their surfaces being covered with PEG and they tended to self-assemble into FONs, with the AIE dye as the hydrophobic core and PEG as the hydrophilic shell. Owing to the introduction of a TPEA AIE dye, such FONs also showed excellent fluorescence in aqueous solution. TPEA-PEG FONs were biocompatible enough for bioimaging applications according to the biocompatibility evaluation. In view of the controllability of RAFT polymerization and the convenience of the Schiff base reaction, many AIE based FONs can also be prepared by employing different AIE dyes. More importantly, various multifunctional FONs can also be easily fabricated for bioimaging applications by further conjugation with other components such as drugs, imaging agents, and targeting agents. In a word, the one-pot strategy combining RAFT polymerization and the Schiff base technology provides an economical and efficient avenue for the preparation of numerous AIE-based FONs, which are promising candidates for various biomedical applications.

Acknowledgements

This research was supported by the National Science Foundation of China (no. 21474057, 21104039, 21134004, 51363016), and the National 973 Project (no. 2011CB935700), the Natural Science Foundation of Guangdong Province (S2013010013580).

References

- 1 J. Geng, J. Lindqvist, G. Mantovani and D. Haddleton, *Angew. Chem., Int. Ed.*, 2008, **47**, 4180–4183.
- 2 P. Golas and K. Matyjaszewski, *Chem. Soc. Rev.*, 2010, **39**, 1338–1354.
- 3 L. Mespouille, M. Vachaud, F. Suriano, P. Gerbaux, O. Coulembier, P. Degée, R. Flammang and P. Dubois, *Macromol. Rapid Commun.*, 2007, **28**, 2151–2158.

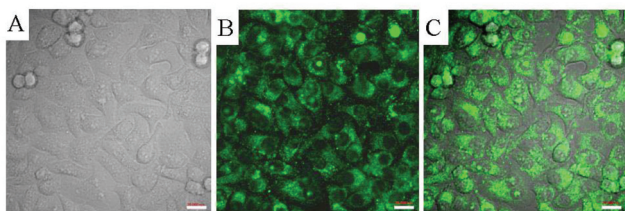


Fig. 4 CLSM images of A549 cells incubated with $20 \mu\text{g mL}^{-1}$ of TPEA-PEG FONs. (A) Bright field, (B) excited with a 405 nm laser, (C) merged image of (A) and (B). Scale bar = $20 \mu\text{m}$.

- 4 B. van As, P. Thomassen, B. Kalra, R. Gross, E. Meijer, A. Palmans and A. Heise, *Macromolecules*, 2004, **37**, 8973–8977.
- 5 F. Wolf, N. Friedemann and H. Frey, *Macromolecules*, 2009, **42**, 5622–5628.
- 6 C. Fu, C. Zhu, S. Wang, H. Liu, Y. Zhang, H. Guo, L. Tao and Y. Wei, *Polym. Chem.*, 2013, **4**, 264–267.
- 7 S. Wang, C. Fu, Y. Zhang, L. Tao, S. Li and Y. Wei, *ACS Macro Lett.*, 2012, **1**, 1224–1227.
- 8 Y. Zhang, C. Fu, C. Zhu, S. Wang, L. Tao and Y. Wei, *Polym. Chem.*, 2013, **4**, 466–469.
- 9 C. Zhu, B. Yang, Y. Zhao, C. Fu, L. Tao and Y. Wei, *Polym. Chem.*, 2013, **4**, 5395–5400.
- 10 Y. Wang, Y. Zhang, F. Zhang and W. Li, *J. Mater. Chem.*, 2011, **21**, 6556–6562.
- 11 C. Shen, W. Yao and Y. Lu, *J. Nanopart. Res.*, 2013, **15**, 2019–2033.
- 12 C. Gazon, J. Rieger, R. Méallet-Renault, G. Clavier and B. Charleux, *Macromol. Rapid Commun.*, 2011, **32**, 699–705.
- 13 R. Sauer, A. Turshatov, S. Balushev and K. Landfester, *Macromolecules*, 2012, **45**, 3787–3796.
- 14 Y. Xin and J. Yuan, *Polym. Chem.*, 2012, **3**, 3045–3055.
- 15 B. Yang, Y. Zhang, X. Zhang, L. Tao, S. Li and Y. Wei, *Polym. Chem.*, 2012, **3**, 3235–3238.
- 16 Y. Zhang, L. Tao, S. Li and Y. Wei, *Biomacromolecules*, 2011, **12**, 2894–2901.
- 17 M. Bentley, M. Roberts and J. Harris, *J. Pharm. Sci.*, 1998, **87**, 1446–1449.
- 18 B. Droumaguet and J. Nicolas, *Polym. Chem.*, 2010, **1**, 563–598.
- 19 L. Tao, G. Mantovani, F. Lecolley and D. Haddleton, *J. Am. Chem. Soc.*, 2004, **126**, 13220–13221.
- 20 S. Ryan, X. Wang, G. Mantovani, C. Sayers, D. Haddleton and D. Brayden, *J. Controlled Release*, 2009, **135**, 51–59.
- 21 F. Qiu, C. Tu, R. Wang, L. Zhu, Y. Chen, G. Tong, B. Zhu, L. He, D. Yan and X. Zhu, *Chem. Commun.*, 2011, **47**, 9678–9680.
- 22 R. Hu, N. Leung and B. Tang, *Chem. Soc. Rev.*, 2014, **43**, 4494–4562.
- 23 G. Heo, S. Cho and K. Wooley, *Polym. Chem.*, 2014, **5**, 3555–3558.
- 24 X. Dai, C. Hong and C. Pan, *Macromol. Chem. Phys.*, 2012, **213**, 2192–2200.
- 25 A. Louie, *Chem. Rev.*, 2010, **110**, 3146–3195.
- 26 X. Zhang, J. Hui, B. Yang, Y. Yang, D. Fan, M. Liu, L. Tao and Y. Wei, *Polym. Chem.*, 2013, **4**, 4120–4125.
- 27 X. Zhang, X. Zhang, B. Yang, M. Liu, W. Liu, Y. Chen and Y. Wei, *Polym. Chem.*, 2014, **5**, 356–360.
- 28 X. Zhang, M. Liu, B. Yang, X. Zhang, Z. Chi, S. Liu, J. Xu and Y. Wei, *Polym. Chem.*, 2013, **4**, 5060–5064.
- 29 X. Zhang, X. Zhang, B. Yang, J. Hui, M. Liu, W. Liu, Y. Chen and Y. Wei, *Polym. Chem.*, 2014, **5**, 689–693.
- 30 X. Zhang, X. Zhang, B. Yang, J. Hui, M. Liu, Z. Chi, S. Liu, J. Xu and Y. Wei, *Polym. Chem.*, 2014, **5**, 683–688.
- 31 X. Zhang, Z. Chi, H. Li, B. Xu, X. Li, W. Zhou, S. Liu, Y. Zhang and J. Xu, *Chem. – Asian J.*, 2011, **6**, 808–811.
- 32 X. Zhang, Z. Chi, H. Li, B. Xu, X. Li, S. Liu, Y. Zhang and J. Xu, *J. Mater. Chem.*, 2011, **21**, 1788–1796.
- 33 X. Zhang, Z. Chi, B. Xu, C. Chen, X. Zhou, Y. Zhang, S. Liu and J. Xu, *J. Mater. Chem.*, 2012, **22**, 18505–18513.
- 34 X. Zhang, M. Liu, B. Yang, X. Zhang and Y. Wei, *Colloids Surf., B*, 2013, **112**, 81–86.
- 35 L. Tao, J. Liu and T. Davis, *Biomacromolecules*, 2009, **10**, 2847–2851.
- 36 X. Zhang, J. Yin, C. Peng, W. Hu, Z. Zhu, W. Li, C. Fan and Q. Huang, *Carbon*, 2011, **49**, 986–995.
- 37 X. Zhang, M. Liu, B. Yang, X. Zhang and Y. Wei, *Colloids Surf., B*, 2013, **112**, 81–86.
- 38 X. Zhang, H. Qi, S. Wang, L. Feng, Y. Ji, L. Tao, S. Li and Y. Wei, *Toxicol. Res.*, 2012, **1**, 201–205.
- 39 Z. Huang, X. Zhang, X. Zhang, C. Fu, K. Wang, J. Yuan, L. Tao and Y. Wei, *Polym. Chem.*, 2015, **6**, 607–612.
- 40 X. Zhang, S. Wang, C. Fu, L. Feng, Y. Ji, L. Tao, S. Li and Y. Wei, *Polym. Chem.*, 2012, **3**, 2716–2719.
- 41 X. Zhang, X. Zhang, B. Yang, J. Hui, M. Liu, Z. Chi, S. Liu, J. Xu and Y. Wei, *Polym. Chem.*, 2014, **5**, 318–322.
- 42 X. Zhang, X. Zhang, L. Tao, Z. Chi, J. Xu and Y. Wei, *J. Mater. Chem. B*, 2014, **2**, 4398–4414.
- 43 Y. Hong, J. Lam and B. Tang, *Chem. Commun.*, 2009, 4332–4353.
- 44 X. Zhang, Z. Chi, J. Zhang, H. Li, B. Xu, X. Li, S. Liu, Y. Zhang and J. Xu, *J. Phys. Chem. B*, 2011, **115**, 7606–7611.
- 45 X. Zhang, M. Liu, B. Yang, X. Zhang, Z. Chi, S. Liu, J. Xu and Y. Wei, *Polym. Chem.*, 2013, **4**, 5060–5064.
- 46 H. Li, X. Zhang, X. Zhang, B. Yang, Y. Yang and Y. Wei, *Polym. Chem.*, 2014, **5**, 3758–3762.